

**Triazine-based Conjugated Microporous Polymers with
N,N,N',N'-Tetraphenyl-1,4-phenylenediamine, 1, 3, 5-
Tris(diphenylamino)benzene and 1,3,5-Tris[(3-methylphenyl)-
phenylamino]benzene as the Core for High Iodine Capture and
Fluorescence Sensing o-Nitrophenol**

Tongmou Geng*, Sainan Ye, Zongming Zhu and Weiyong Zhang

*Collaborative Innovation Center for Petrochemical New Materials, Anhui Province Key
Laboratory of Optoelectronic and Magnetism Functional Material, Anqing Normal University,
Anqing 246011, China*

Corresponding Author:

Tongmou Geng

Mailing Address: School of Chemistry and Chemical Engineering, Anqing Normal University,
Anqing 246011, China

Telephone: +86-0556-5500090

Fax: +86-0556-5500090

E-mail addresses: gengtongmou@aqnu.edu.cn (TM Geng).

EXPERIMENTAL SECTION

Chemicals and reagents

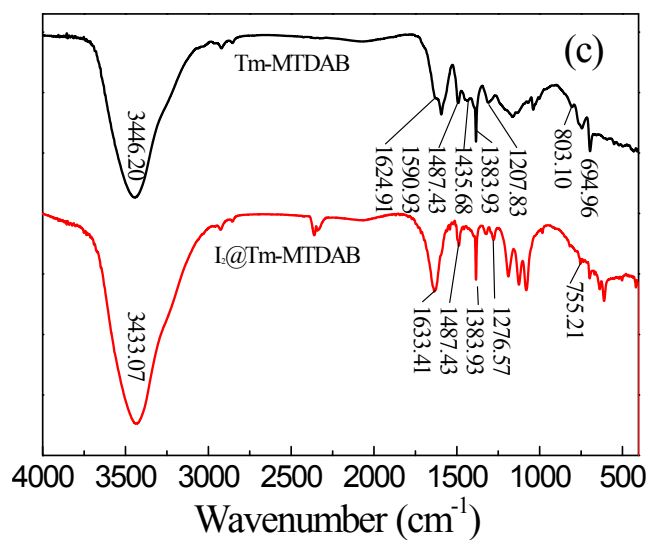
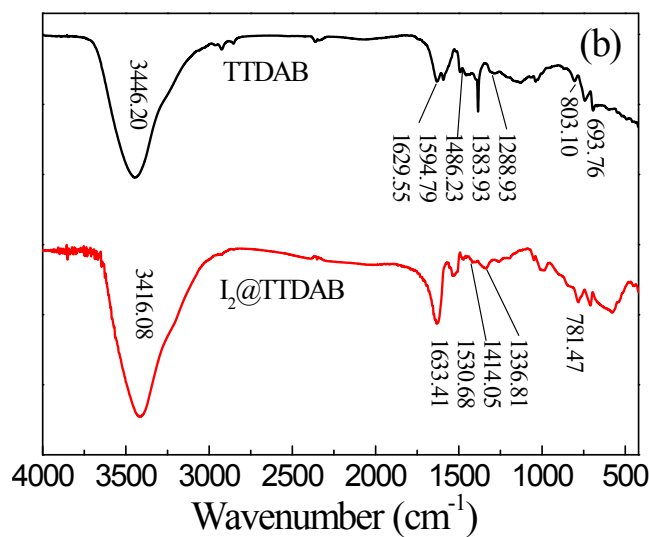
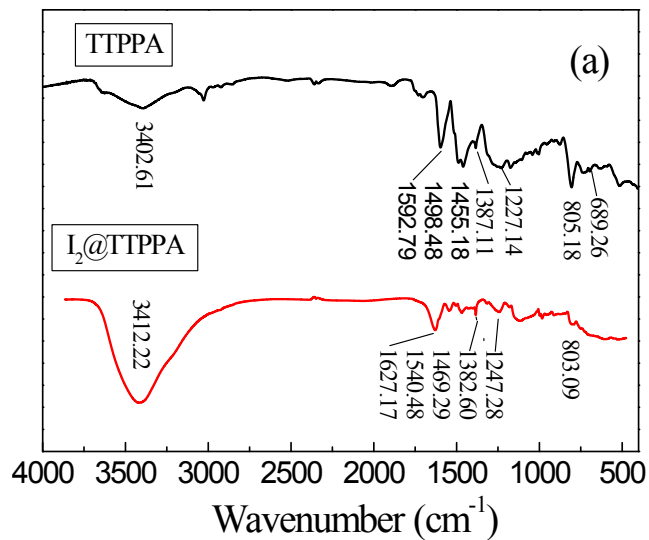
N,N,N',N'-tetraphenyl-1,4-phenylenediamine (TPPA) 1,2-dichlorobenzene, 2,4,6-trichloro-1,3,5-triazine (TCT), methane-sulfonic acid, and 1,3,5-Tris[(3-methylphenyl)phenylamino]benzene (m-MTDAB) were purchased from Aladdin reagent (Shanghai) Co. Ltd. and used as received. 1,3,5-Tris(diphenylamino)benzene (TDAB) was purchased from Shanghai Zhen Zhun biological science and technology Co. Ltd. and used as received. Unless otherwise noted, all other reagents and solvents were of analytical grade and used as supplied without further purification.

Adsorbent Recycle

Recycling percentage (Rp) of the adsorbents was determined as follows: 30 mg of iodine-equilibrium TCMPs ($I_2@PTPPA$, $I_2@TTDAB$ and $I_2@Tm-MTDAB$) powders were charged in an open glass vial (10 mL) and heated at 398 K for 120 min in air dry oven. The recovered TCMPs powders were reused for iodine uptake at 350 K for 22 h. The recycling percentage were calculated by weight gains: $R_p = \frac{C_u}{C_{u_0}} \times 100 \text{ wt } \%$, where Rp is the recycling percentage, C_{u_0} and C_u are the iodine uptake capacity of TCMPs before and after heating recovered. The same powders were recycled three times. The above-mentioned iodine uptake, release, and recycling percentage of adsorbents were average values that obtained from three measurements each. (*Macromolecules* 2016, 49, 6322–6333.)

Measurements

The infrared spectra were recorded from 400 to 4000 cm^{-1} on an iS50FT-IR spectrometer by using KBr pellets. Solid-state ^{13}C CP/MAS NMR measurements were recorded on a Bruker AVANCE III 400 WB spectrometer at a MAS rate of 5 kHz and a CPcontact time of 2 ms. Elemental analyses were carried out on a VARIO ELIII cube analyzer. UV–Vis spectra were recorded on an UV-2501PC spectrometer. Scanning electron microscopy was performed on a S-3400N microscope. X-ray diffraction data were recorded on a XRD600 diffractometer by depositing powder on glass substrate, from $2\theta = 5^\circ$ up to 90° with 0.02° increment. Thermogravimetric analysis (TGA) measurements were performed on a CDR-4P TGA under N_2 , by heating to 800°C at a rate of $10^\circ\text{C min}^{-1}$. The Brunauer-Emmett-Teller (BET) method was utilized to calculate the specific surface areas and pore volume, the Saito-Foley (SF) method was applied for the estimation of pore size distribution. Raman spectra were acquired using a DXR equipped with a 532 nm diode laser. Fluorescence spectra were recorded on a RF-5301PC spectrophotometer (Shimadzu). The samples were prepared as follows: dried CMPs powder (10 mg) ground with an agate mortar was added to 10 mL of organic solvents. After the resulting mixture was well dispersed with ultrasound, the dispersion colloid was obtained.



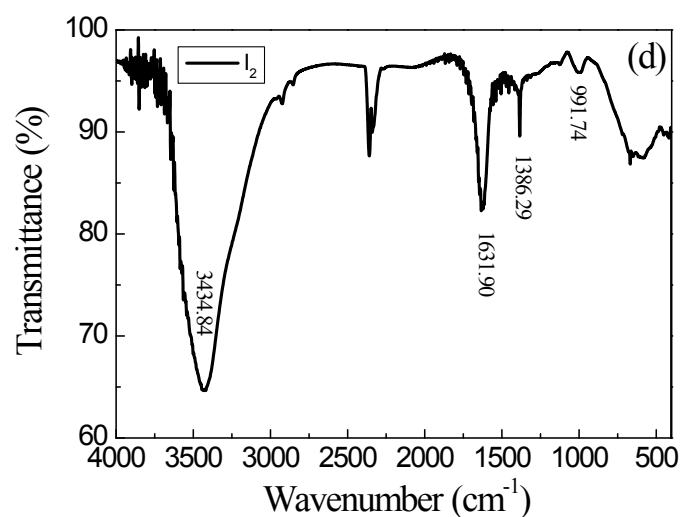


Fig. S1. FT-IR spectra of CMPs, iodine-loaded CMPs and pristine iodine. (a) TTPPA, $I_2@TTPPA$; (b) TTDAB, $I_2@TTDAB$; (c) Tm-MTDAB, $I_2@Tm-MTDAB$ and (d) I_2 .

Table S1. Elemental analysis data of TTPPA, TTDAB and Tm-MTDAB

wt%		C	H	N
TTPPA	Anal. calcd.	79.67	3.933	16.40
	Found	78.63	4.859	14.86
TTDAB	Anal. calcd.	85.27	4.442	10.29
	Found	82.89	4.427	9.949
Tm-MTDAB	Anal. calcd.	84.90	5.516	9.582
	Found	82.10	5.029	10.21

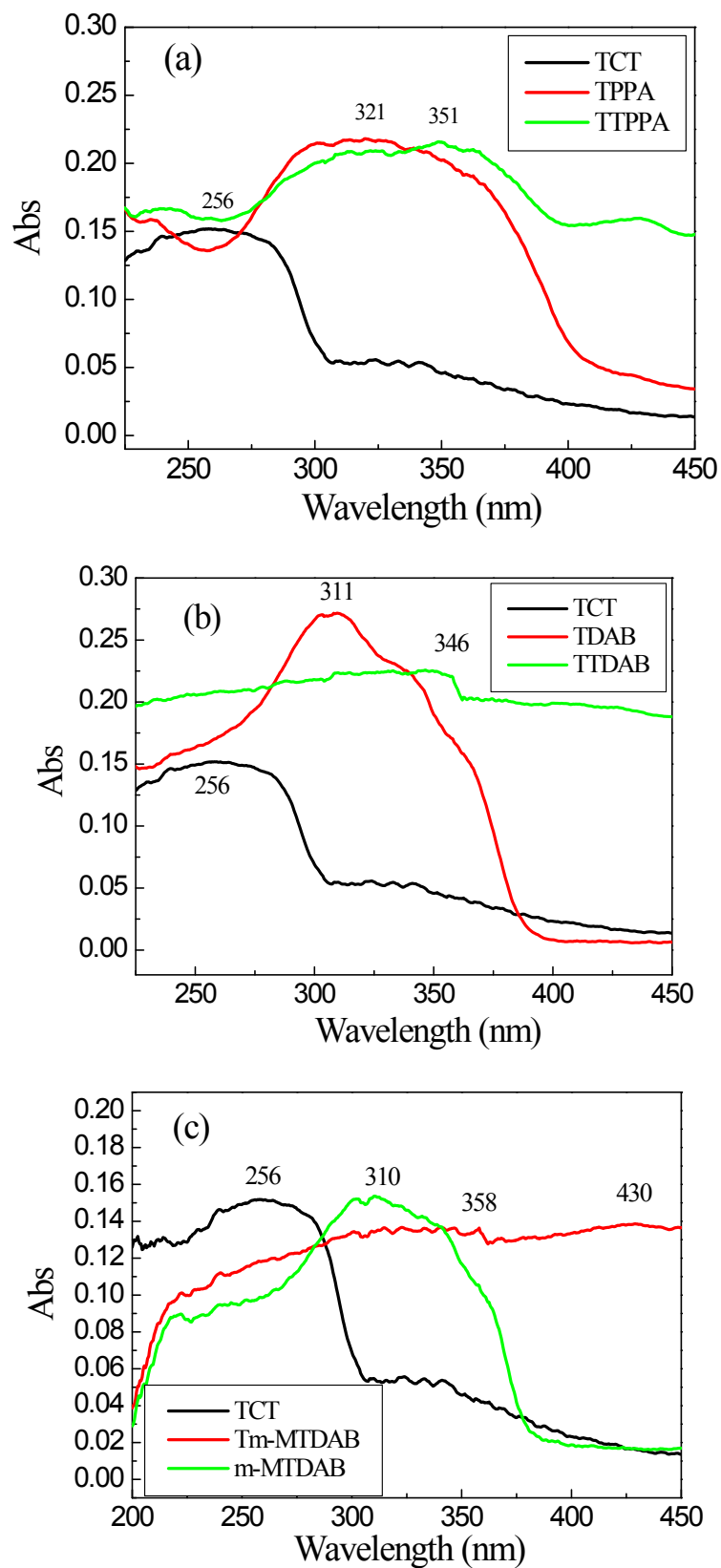


Fig. S2. UV-Vis spectra of the solid-states of TCT, monomers and TCMPs. (a) TTPPA, (b) TTDAB and (c) Tm-MTDAB.

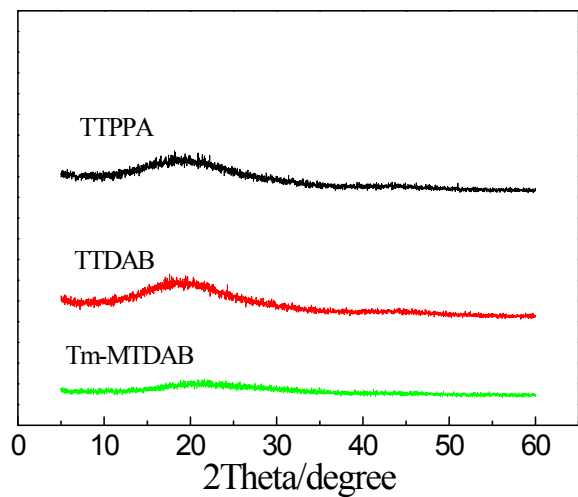


Fig. S3. XRD patterns of TTPPA, TTDAB and Tm-MTDAB.

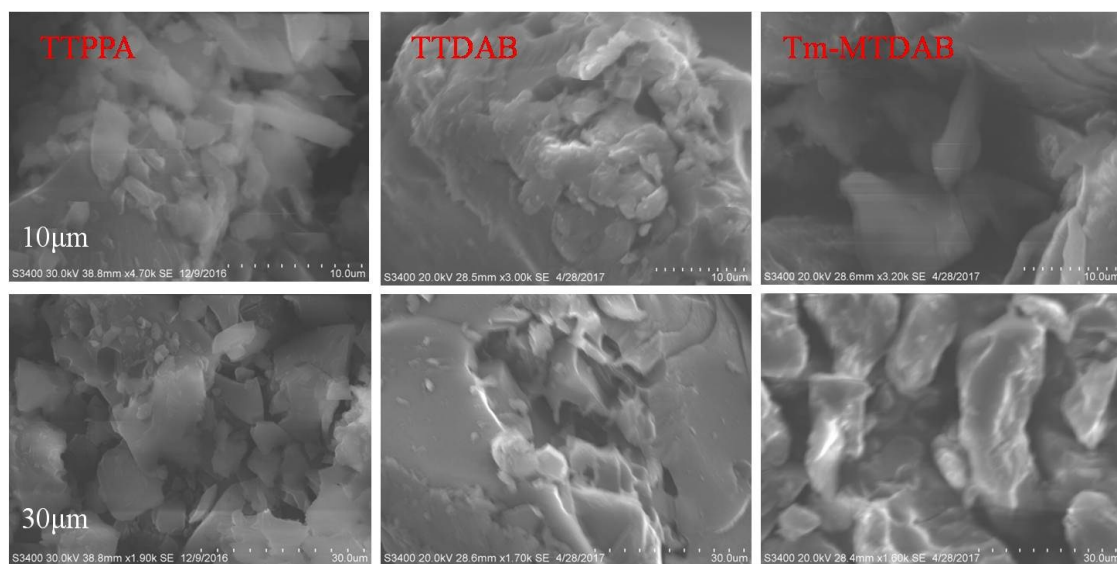


Fig. S4. The representative SEM micrographs of TTPPA, TTDAB, and Tm-MTDAB.

Scale: top: 10 μm, bottom: 30 μm.

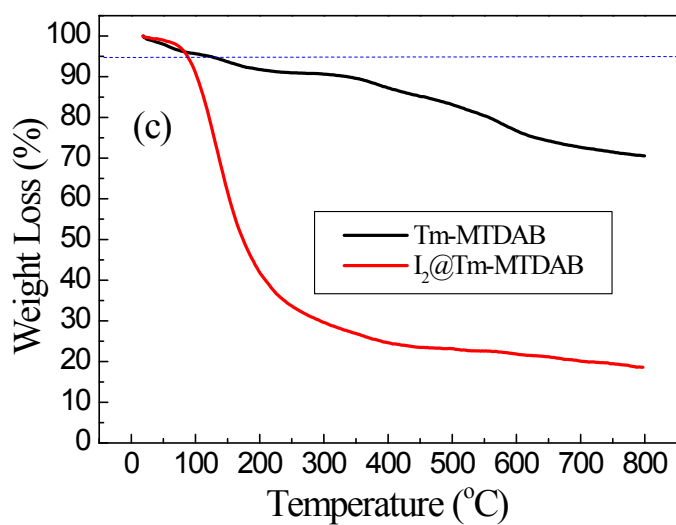
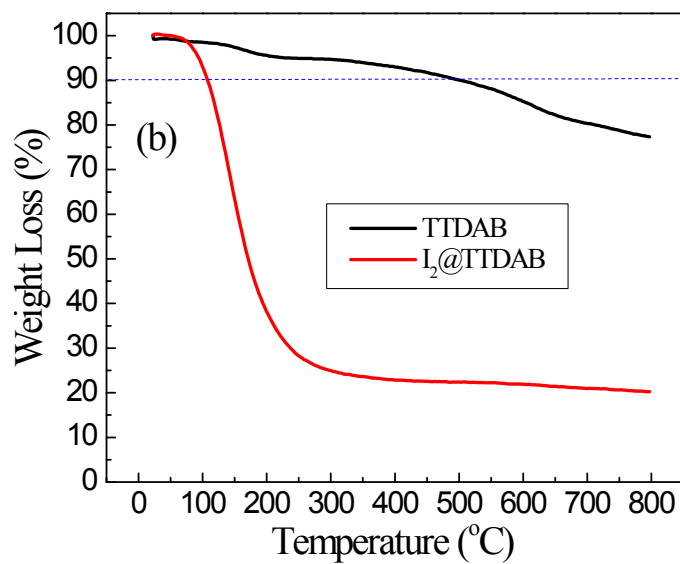
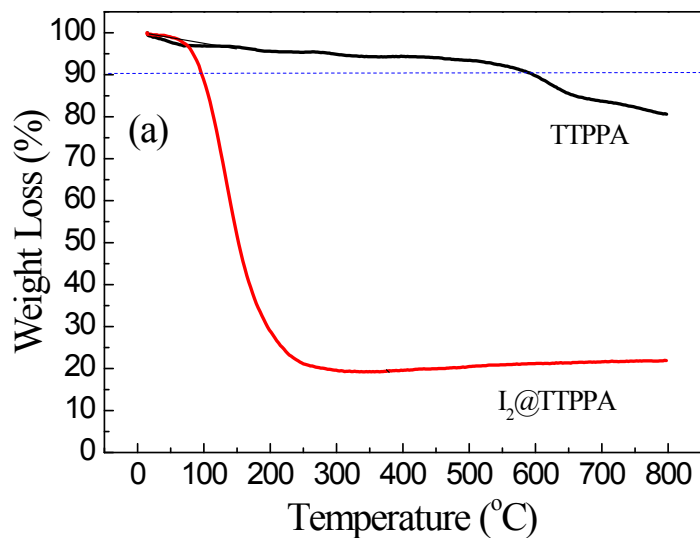


Fig. S5. Thermogravimetric analysis (TGA) curves of (a) TTPPA and I₂@TTPPA, (b) TTDAB and I₂@TTDAB, (c) Tm-MTDAB and I₂@Tm-MTDAB.

Table S2 Pore and surface properties of TTPPA, TTDAB and Tm-MTDAB.

TCMPs	$S_{\text{BET}}^{\text{a}}$	$S_{\text{Langmuir}}^{\text{a}}$	V_{total}	$V_{\text{micro}}^{\text{c}}$	$V_{\text{micro}}/$	$S_{\text{micro}}^{\text{c}}$	$S_{\text{external}}^{\text{c}}$
	($\text{m}^2 \text{g}^{-1}$)	($\text{m}^2 \text{g}^{-1}$)	(tpv) ^b	($\text{cm}^3 \text{g}^{-1}$)	V_{total}	($\text{m}^2 \text{g}^{-1}$)	($\text{m}^2 \text{g}^{-1}$)
			($\text{cm}^3 \text{g}^{-1}$)				
PTPPA	512.39	690.99	0.2997	0.1254	41.84	274.84	237.56
TTDAB	1.643	2.393	0.004	0	0	0	1.643
Tm-MTDAB	2.778	4.843	0.007	0	0	0	2.778

^a Specific surface area calculated from the adsorption branch of the nitrogen isotherm using the BET method in the relative pressure (P/P_0) range from 0.01 to 0.10.

^b Total pore volume is obtained from BET data up to $P/P_0=0.97$ and is defined as the sum of micropore volume and volumes of larger pores.

^c Micropore volume calculated from nitrogen adsorption isotherm using the t-plot method.

Table S 3. Summary of surface area and iodine sorption properties of CMPs.

Sample	BET	T (°C)	Iodine uptake	Ref
(heteroatom)	($\text{m}^2 \text{g}^{-1}$)		(g g^{-1})	
NiP-CMPs	2600	77	2.02	<i>Chem. Commun.</i> 2014, 50,
(N)				8495-8498.
PAF-1, JUC-Z2	5600,	25	1.86, 1.44	<i>J. Mater. Chem. A</i> , 2014, 2,
(no N, S)	2081			7179–7187.
CMPN-1, CMPN-2,	1368	70.3	0.97, 1.10,	<i>J. Mater. Chem. A</i> , 2015, 3, 87–

CMPN-3 (no N, S)			2.08	91.
PAF-23, PAF-24,	82, 136,	75	2.71, 2.76,	<i>Angew. Chem. Int. Ed.</i> , 2015,
PAF-25 (B, Li ⁺)	262		2.60	54, 12733 –12737.
Azo-Trip	510.4	77	2.33	<i>Polym. Chem.</i> , 2016, 7, 643–
(N)				647.
SCMP-1, SCMP-2	413, 855	80	1.88, 2.22	<i>ACS Appl. Mater. Interfaces</i> ,
(S)				2016, 8, 21063–21069.
SCMP-I, SCMP-II	2.72,	80	3.45	<i>Chem. Commun.</i> , 2016, 52,
(S)	119.76			9797-9800.
Por-Py-CMP	1014	77	1.30	<i>RSC Adv.</i> , 2016, 6, 75478–
(N)				75481.
HCMP-1, -2, -3, -4	430, 153,	85	1.59, 2.81,	<i>Macromolecules</i> , 2016, 49,
(N)	82, n.a.		3.16, 2.22	6322–6333.
NTP	1067	75	1.80	<i>ACS Macro Lett.</i> , 2016, 5,
(N)				1039–1043.
N APOP-1,-2,-3,-4	657, 458,	75	2.06,2.39,	<i>J. Polym. Sci., Part A: Polym.</i>
(N)	702, 626		2.41,2.65	<i>Chem.</i> 2016, 54, 1724–1730.
COP ₁ ⁺⁺ , COP ₁ ⁺ ,	-	60	2.12, 1.95,	<i>J. Mater. Chem. A</i> , 2016, 4(4):
COP ₁ ⁰ ,COP ₂ ⁺⁺ ,			3.80,2.58,	15361-15369.
COP ₂ ⁺ , COP ₂ ⁰ (N)			2.11,2.77	
BQCMP-1,	422	80	1.51	<i>Macromol. Mater. Eng.</i> 2016,
BQCMP-2 (N)	123		1.61	301, 1104–1110.

AzoPPN (N)	400	77	2.90	<i>Chem. Eur. J.</i> , 2016, 22(33), 11863–11868.
POP-1,POP-2 (N)	12,41	80	3.57, 3.82	<i>J. Hazard. Mater.</i> 2017, 338, 224–232.
TTPB (N)	222	77	4.43	<i>J. Mater. Chem. A</i> , 2017, 5, 7612–7617
FCMP-600@1-4 (F)	551, 636, 692, 88	77	1.08, 1.41 0.90, 1.11	<i>Sci Rep</i> , 2017, 7(1): 13972-.
NCMP1, NCMP2, NCMP3 (N)	58, 280, 485	85	2.15, 1.86, 1.61	<i>ACS Appl. Mater. Interfaces</i> , 2017, 1944-8244.
TTPPA(N)	512	77	4.90	This work.
TTDTPA(N)	1.643	77	3.13	This work.
TTMTPA(N)	2.778	77	3.04	This work.

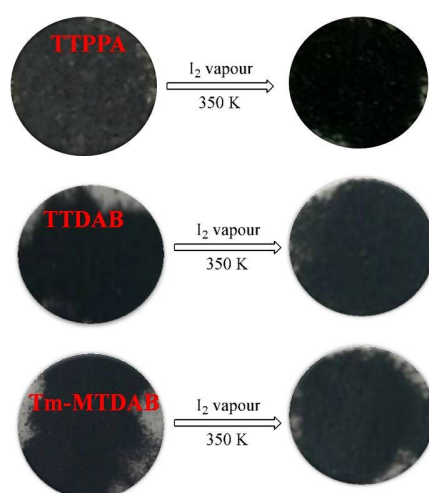


Fig. S6. Photographs showing the color changes before and after iodine capture for TTPPA, TTDAB, and Tm-MTDAB.

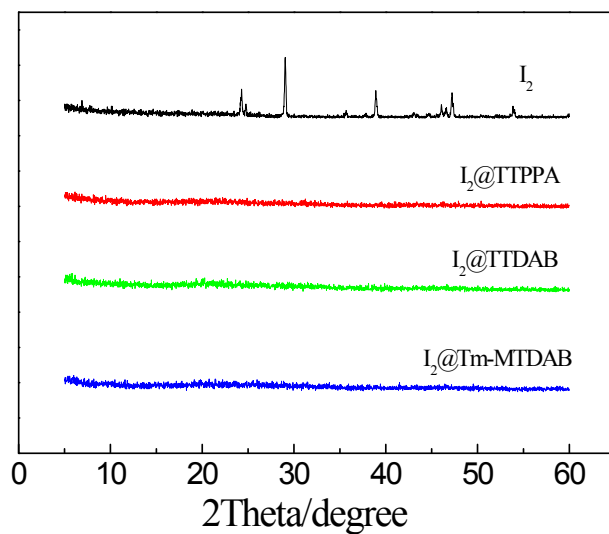


Fig. S7. XRD patterns of I_2 , $I_2@TTPPA$, (b) $I_2@TTDAB$ and $I_2@Tm-MTDAB$.

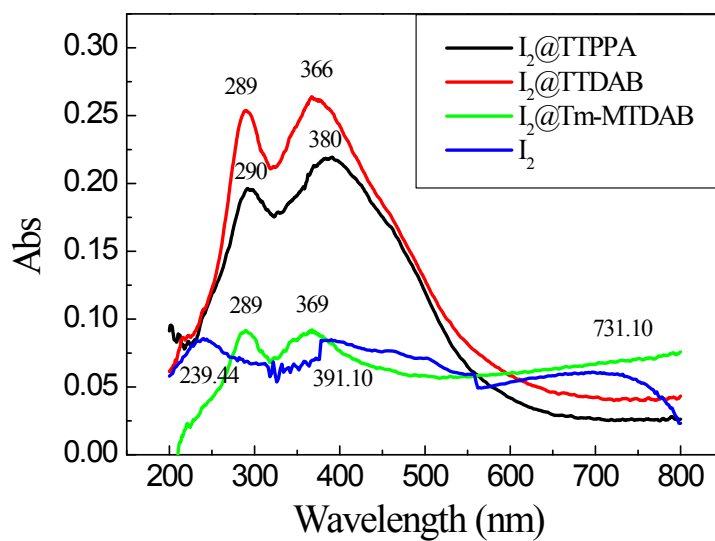


Fig. S8. UV-Vis spectra of $I_2@TTPPA$, $I_2@TTDAB$, $I_2@Tm-MTDAB$, and I_2 .

Table S4. The peak shifts of FT-IR spectra of parents and iodine-loaded TCMPs

	TTPPA(2)	$I_2@TTPPA$	shift
triazine, C=N	1593	1627	34

triazine, C-N	1387	1469	82
C-N	1227	1383	156
triazine, benzene ring: in-plane	1498	1540	42
triazine, benzene ring: out-of-plane	805	803	-2
H ₂ O	3403	3412	9
	TTDAB	I ₂ @ TTDAB	peak shift
triazine, C=N	1594.79	1633.41	38.62
triazine, benzene ring: in-plane	1486.23	1530.68	44.45
triazine, C-N	1383.93	1414.05	30.12
C-N	1288.93	1336.81	47.88
triazine, benzene ring: out-of-plane	803.10	781.47	-21.63
H ₂ O	3446.20	3416.08	-30.12
	Tm-MTDAB	I ₂ @Tm-MTDAB	peak shift
triazine, C=N	1590.93	1633.41	42.48
triazine, C-N	1383.93	1487.43	103.5
triazine, benzene ring: in-plane	1435.68	1487.43	51.75
C-N	1207.83	1383.93	68.74
triazine, benzene ring: out-of-plane	803.10	755.21	-47.89
H ₂ O	3446.20	3433.07	-13.13

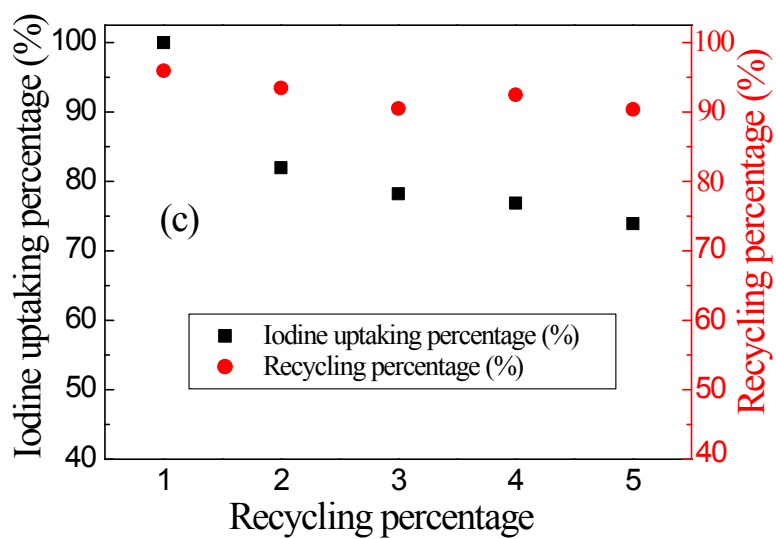
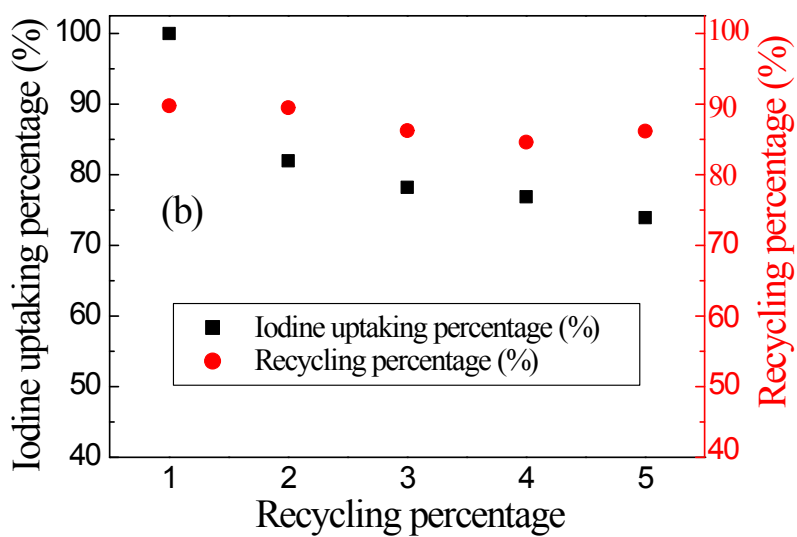
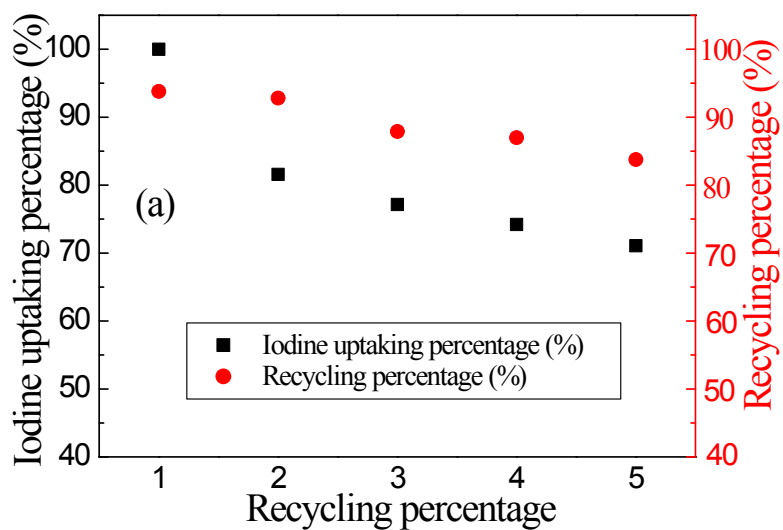


Fig. S 9. Recycling percentage of (a) TTPPA, (b) TTDAB and (c) Tm-MTDAB

(recycling parameters: 1.0 bar, 350 K, 22 h and 398 k, 120 min).

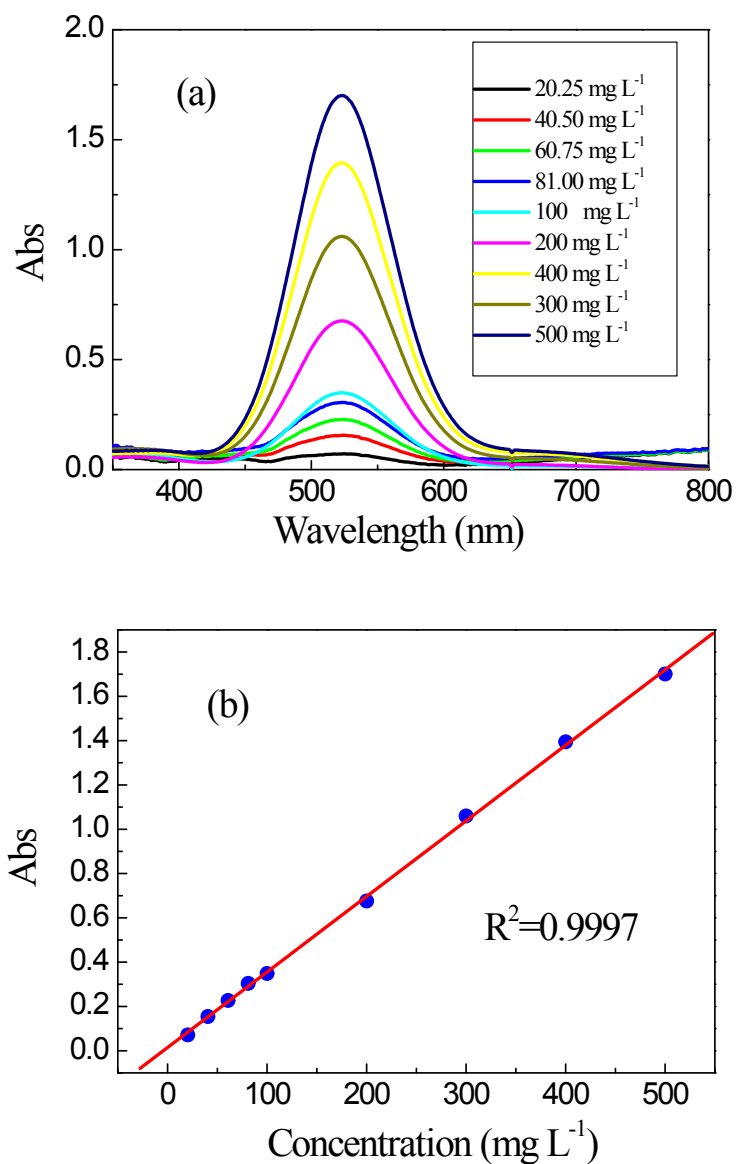


Fig. S10. (a) Calibration plot of standard iodine by UV-Vis spectra in cyclohexane solution. (b) The fitting of Abs value vs concentration of I₂ with the relatively good linearity satisfies Lambert-Beer Law.

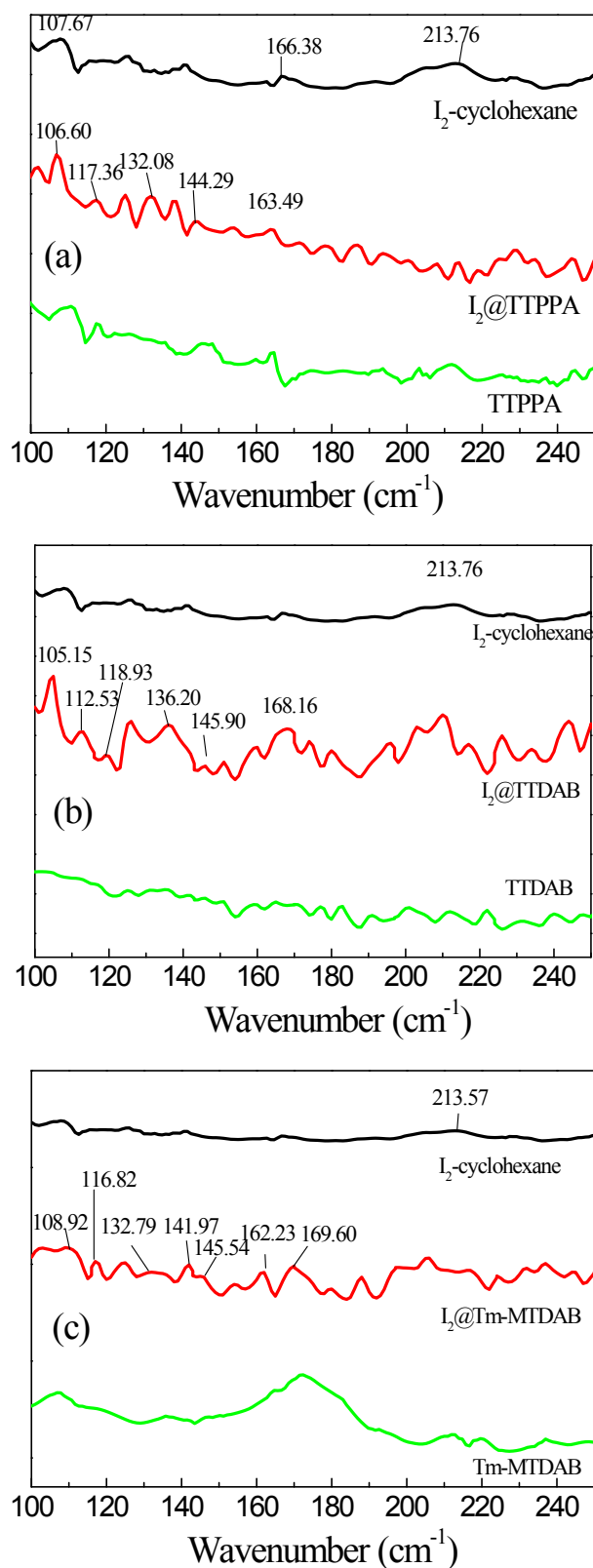


Fig. S11. Raman spectra of iodine–cyclohexane solution (black), iodine-loaded TCMPs obtained by iodine sorption in cyclohexane solution (red) and TCMPs (green); (a) TTPPA, (b) TTDAB and (c) Tm-MTDAB.

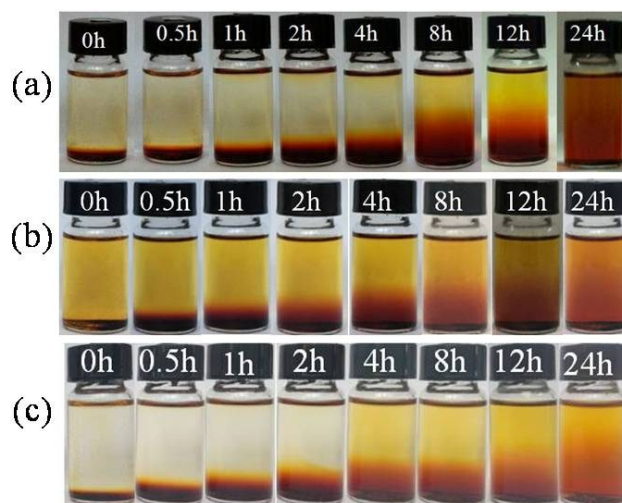
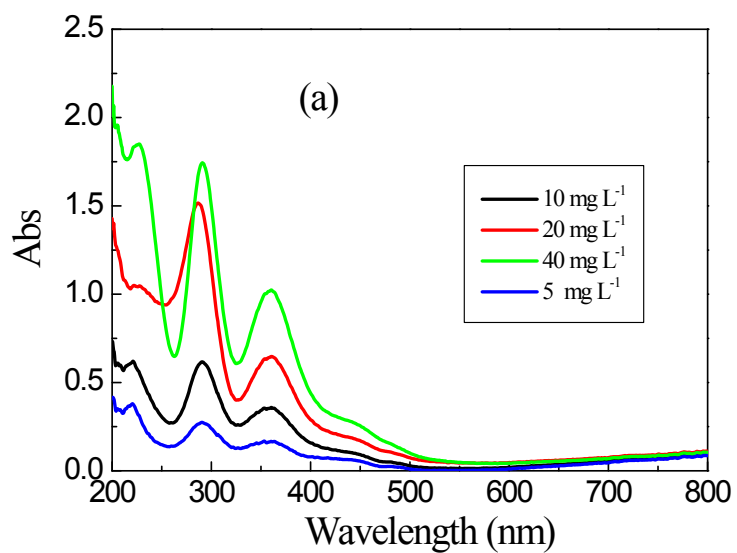


Fig. S12. Photographs showing progress of the iodine release from (a) $I_2@TTPPA$, (b) $I_2@TTDAB$ and (c) $I_2@Tm-MTDAB$, respectively, when the containing iodine polymer networks were immersed in ethanol.



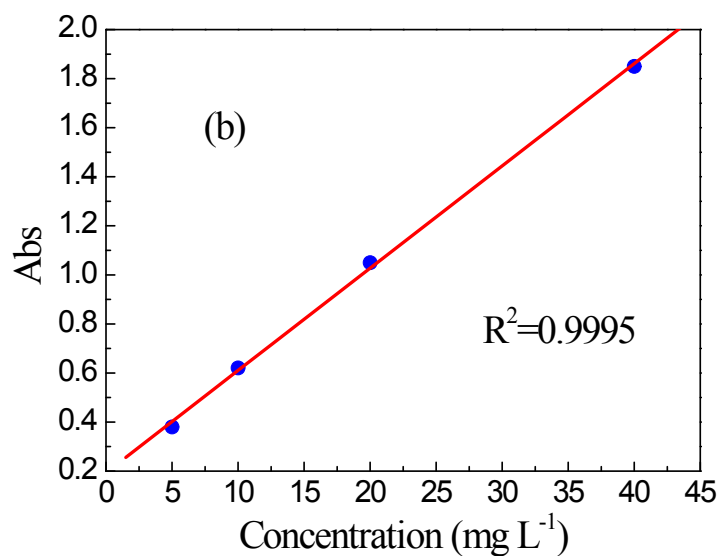


Fig. S13. (a) Calibration plot of standard iodine by UV-Vis spectra in ethanol solution.

(b) The fitting of Abs value vs concentration of I₂ with the relatively good linearity satisfies Lambert-Beer Law.

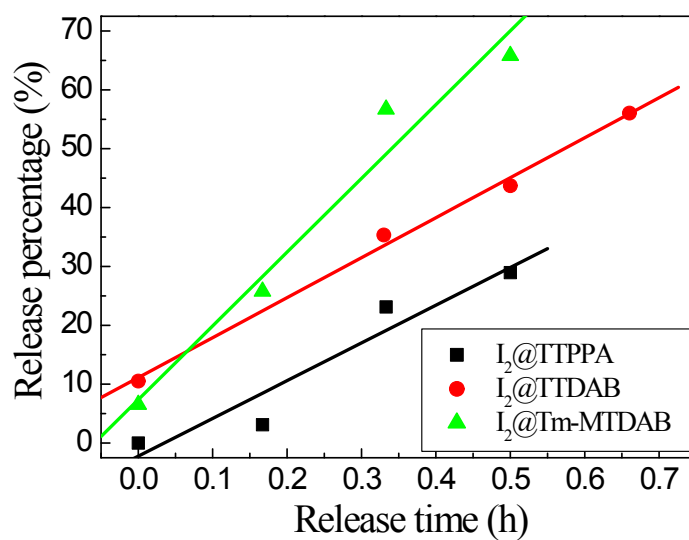


Fig. S14. Controlled release rate of iodine in TTPPA, TTDAB and Tm-MTDAB in the first 30 min determined by UV-Vis absorbance at 291 nm.

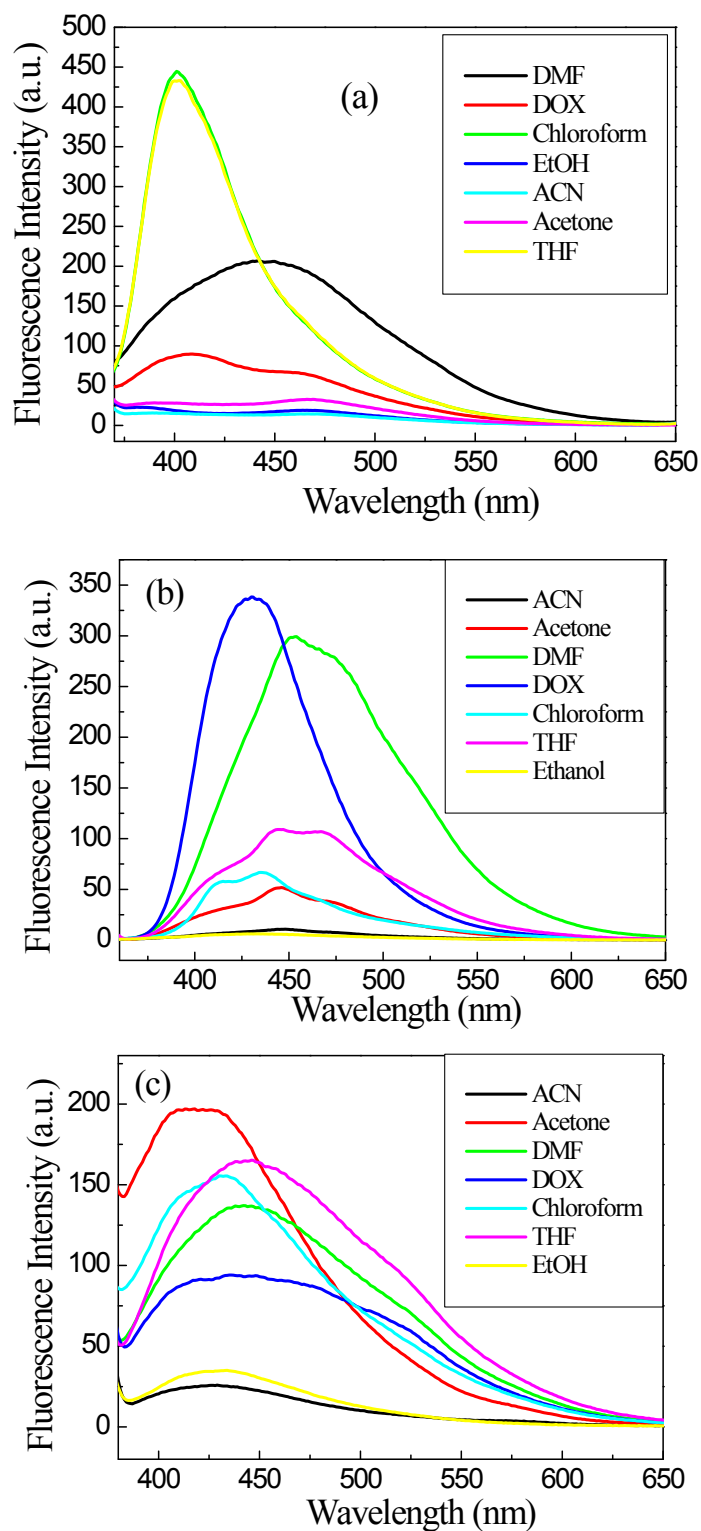


Fig. S15. Fluorescence emission spectra of (a) TTPPA, (b) TTDAB, and (c) Tm-MTDAB suspended in varying polar solvent: ACN, acetone, DMF, DOX, chloroform, THF, and ethanol, respectively, excited with the wavelength of 340, 340 and 350 nm, respectively.

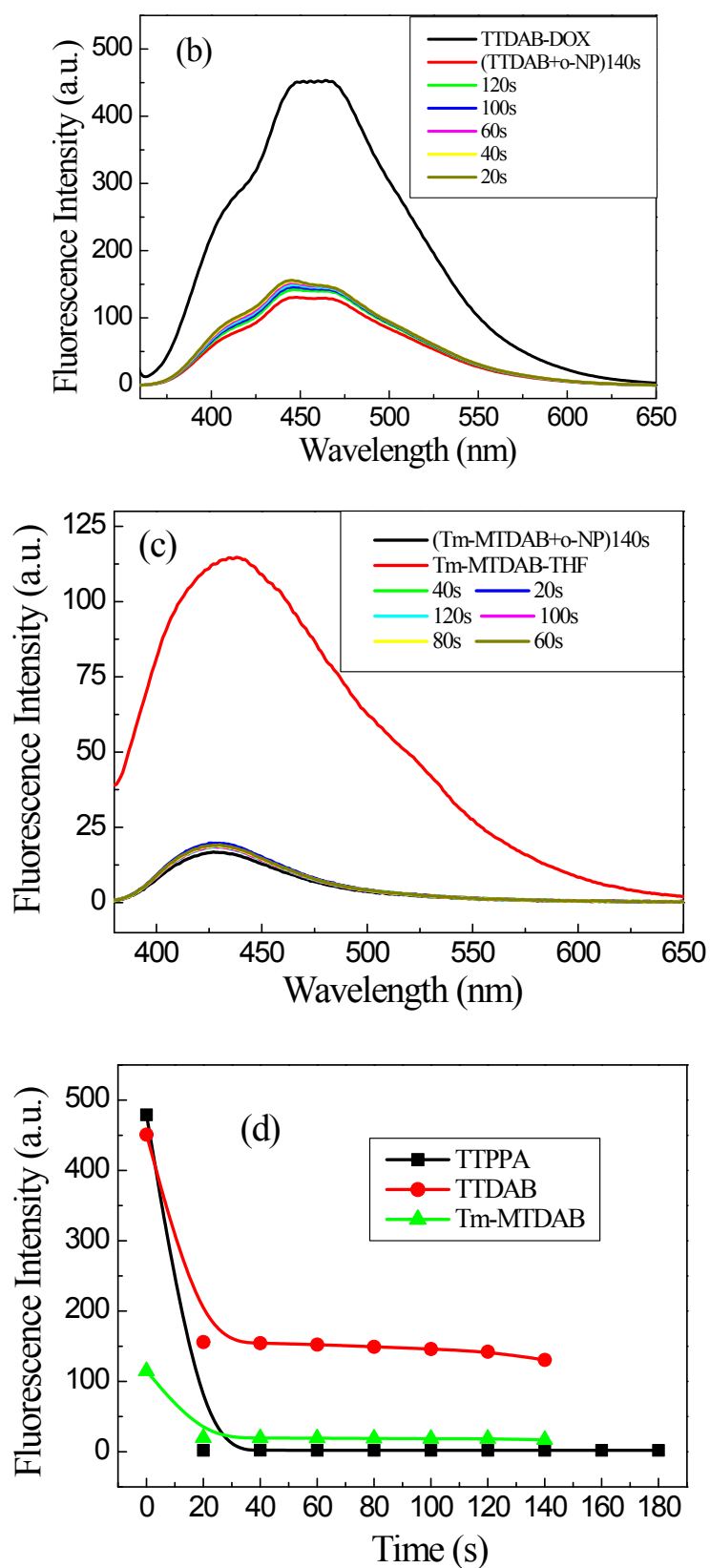
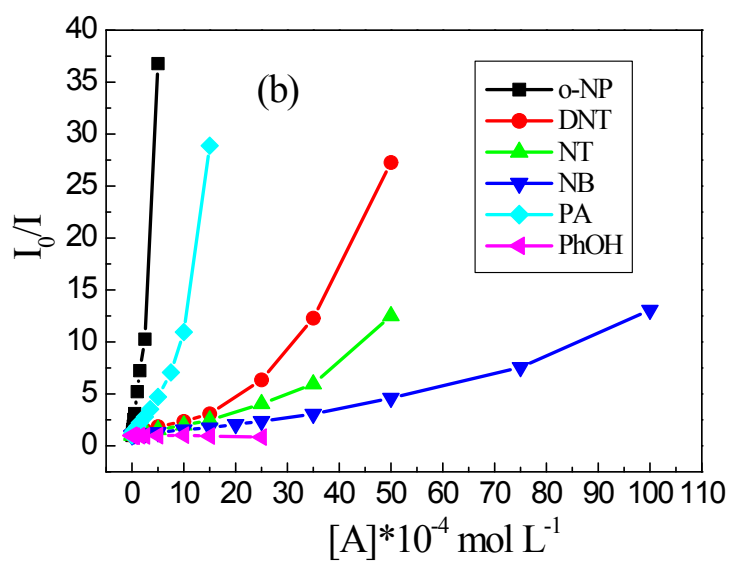
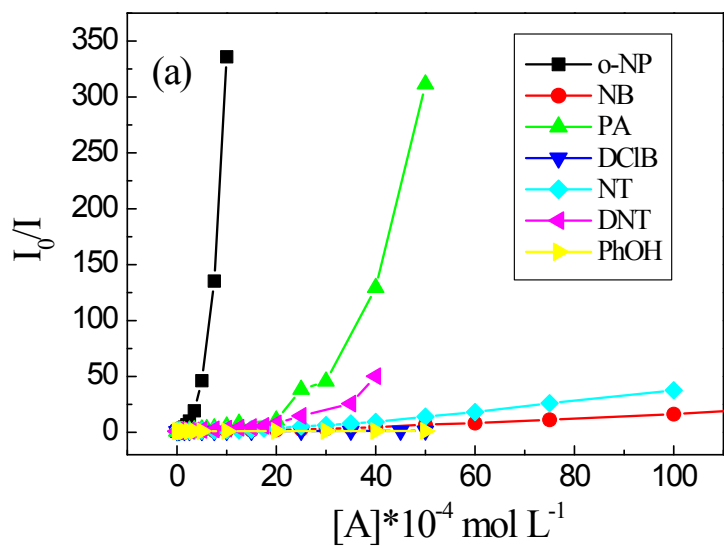


Fig. S17. Fluorescence spectral changes of (a) TTPPA, (b) TTDAB, and (c) Tm-MTDAB upon addition of o-NP of 5.0×10^{-4} mol L⁻¹ with time. (d) The curves are the

evolution of maximum photolumumescence intensity as a function of time. The excitation wavelength was 340, 340 and 350 nm, respectively.



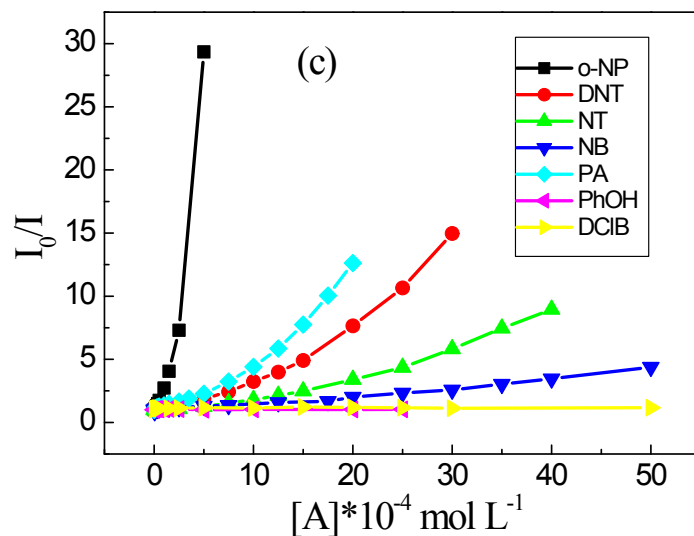


Fig. S18. The plots of I_0/I against varying NACs concentrations. Polymer concentrations: 1.0 mg L^{-1} . (a) TTPPA in THF ($\lambda_{\text{ex}}=340 \text{ nm}$), (b) TTDAB in DOX ($\lambda_{\text{ex}}=340 \text{ nm}$), (c) Tm-MTDAB in THF ($\lambda_{\text{ex}}=350 \text{ nm}$).

Table S4. The equation of I_0/I of TTPPA, TTDAB and Tm-MTDAB to the concentrations of o-NP for suspension in THF or DOX.

CMPs	Solvent	The equation	Regression	The concentration	detection
			coefficient	range of PA	limit
			(R)	(mol L^{-1})	(mol L^{-1})
TTPPA	THF	$I_0/I=1.01+1.19 \times 10^4[o\text{-NP}]$	0.9972	0 to 2.0×10^{-5}	6.32×10^{-10}
TTDAB	DOX	$I_0/I=0.959+2.11 \times 10^4[o\text{-NP}]$	0.9995	0 to 3.0×10^{-4}	1.42×10^{-10}
Tm-MTDAB	THF	$I_0/I=0.947+8.63 \times 10^3[o\text{-NP}]$	0.9969	0 to 2.0×10^{-4}	1.74×10^{-10}

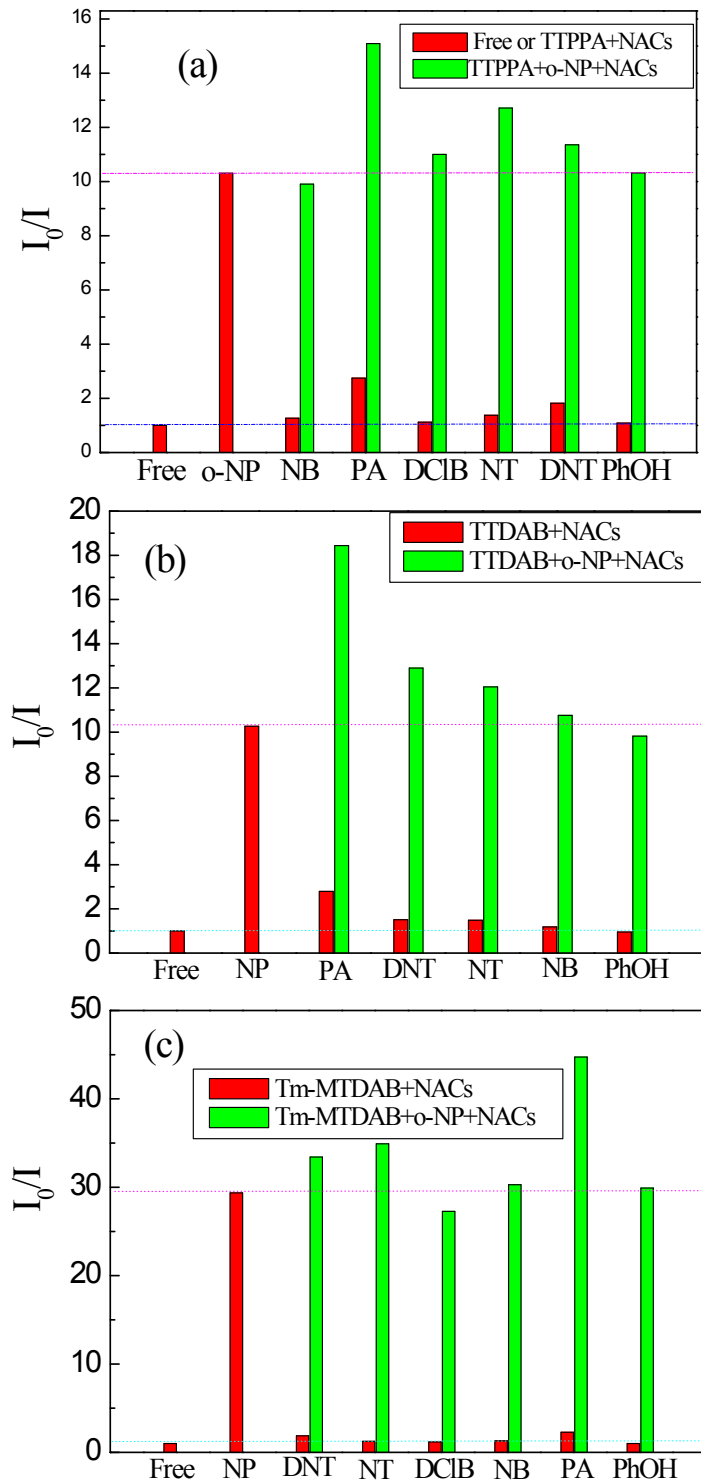


Fig. S19. The PL quenching of three TCPPs for sensing NACs at the same concentration of $5.0 \times 10^{-4} \text{ mol L}^{-1}$ in THF or DOX solutions. (a) TTPPA, (b) TTDAB, and (c) Tm-MTDAB.

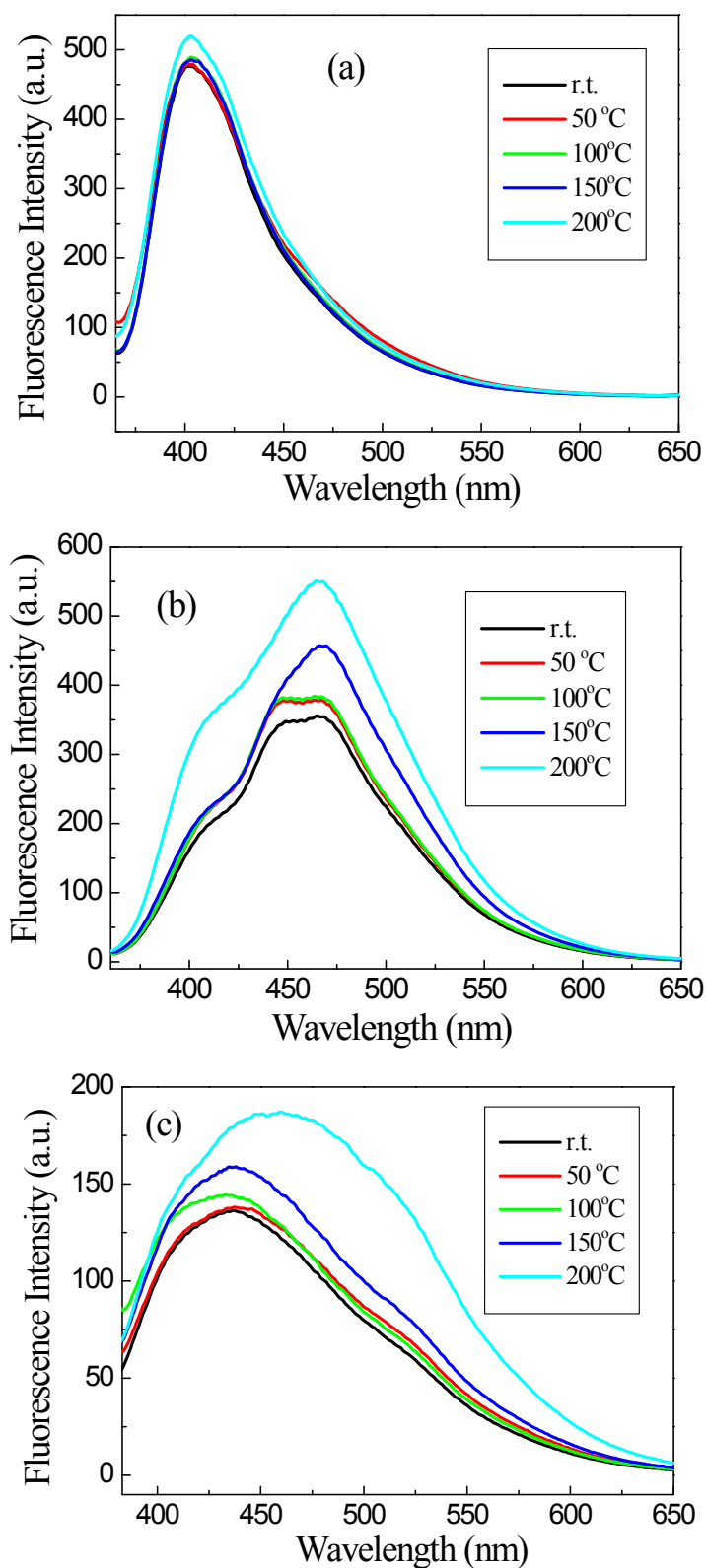


Fig. S20. Fluorescent spectra of (a) TTPPA ($\lambda_{ex}=340$ nm), (b) TTDAB ($\lambda_{ex}=340$ nm), and (c) Tm-MTDAB ($\lambda_{ex}=350$ nm) before and after annealing at different temperatures for 30 min in air.